

Calculation of the Deuteron Quadrupole Relaxation Rate in a Mixture of Water and Dimethyl Sulfoxide

Markus G. Müller,[†] Edme H. Hardy,^{*,†,§} Patrick S. Vogt,[†] Christoph Bratschi,[†]
Barbara Kirchner,^{†,||} Hanspeter Huber,[†] and Debra J. Searles[‡]

*Contribution from the Department of Chemistry, University of Basel,
Klingelbergstr. 80, CH-4056 Basel, Switzerland, and School of Science, Griffith University,
Brisbane, Qld 4111, Australia*

Received November 24, 2003; E-mail: Edme.Hardy@mvm.uni-karlsruhe.de

Abstract: An approach is presented that allows NMR relaxation rates to be determined for a complex mixture, and it is applied to a dimethyl sulfoxide/water solution. This approach is novel for such systems, having only been used for simple systems such as atomic liquids or atomic ions in liquids until now. It involves use of a predetermined, quantum mechanical, multidimensional property surface in a simulation. The results are used in conjunction with the simulated rotational correlation time to calculate the deuteron quadrupole coupling constant (*DQCC*), in an analogous approach to the one used by experimentalists, and to examine the surprising experimental findings for the composition dependence of the *DQCC* in the dimethyl sulfoxide/water mixture. Experiments have suggested that the *DQCC* for a mixture of 5% dimethyl sulfoxide in water is close to the *DQCC* of ice, whereas its value increases to a value close to the gas value with further dilution.¹ The results are further critically analyzed using combinations of different experimental and theoretical results from the literature.

1. Introduction

Aqueous solvation is of both fundamental and practical importance, yet it is still not well understood. Even simple mixtures such as alcohol with water² and dimethyl sulfoxide (DMSO) with water¹ display interesting behavior which are yet to be fully explained.

In 1986, Gordalla and Zeidler (GZ) experimentally found that the deuteron quadrupole coupling constant in a mixture of water and DMSO displayed a curious trend as a function of the composition.¹ The *DQCC* went through a minimum close to its value in ice at a mole fraction of approximately $x_{\text{water}} = 0.95$, then increased to reach a value similar to the gas-phase value at $x_{\text{water}} = 0.30$. Use of molecular dynamics simulations in conjunction with quantum chemical calculations provides an opportunity to both reproduce the experimentally determined results and to explore the reason for the outcome. The trend may be due to a physical change in the structure of the system or an anomaly in the way that the experimental data are treated.

In 2000, we carried out molecular dynamics simulations of the *DQCC* in D₂O in the water/DMSO system at different compositions^{3,4} in an attempt to reproduce the results obtained by GZ. Using snapshots from molecular dynamics simulations

to generate a representative ensemble of configurations of liquid clusters, quantum mechanical calculations of the electric field gradient at the deuteron were carried out. This led directly to an ensemble averaged value of the *DQCC*.³ The calculated values were found to be in the same quantitative range as those observed in the experiment, however the dependence on composition that was determined computationally differed from the experimental results, and the *DQCC* was found to be relatively insensitive to the composition of the mixture.^{3,4} This discrepancy could stem from the approximations used to obtain the experimental *DQCC* from relaxation time measurements or approximations used in the computer simulation. To further investigate the source of the difference, electric field gradient time correlation functions are required. These lead directly to the spin–lattice relaxation times and, if their values are in agreement with the measured values, would suggest that the source of the discrepancy between simulated and experimental results is due to assumptions required in the analysis of the experimental data. In this work we calculate these spin–lattice relaxation times (T_1) and relaxation rates ($R_1 = (T_1)^{-1}$).

DMSO has both polar and nonpolar groups, it has a large dipole moment (4.3 D),⁵ and an oxygen atom that is free to interact with water molecules. Therefore, the liquid structure of mixtures with water is the result of a combination of these effects. The mixture is by far not ideal, but the strongest deviations are usually found at mole fractions around 0.5 ±

[†] Department of Chemistry, University of Basel.

[‡] School of Science, Griffith University.

[§] Present address: Institut für Mechanische Verfahrenstechnik und Mechanik, Bereich angewandte Mechanik/Forscherguppe NMR, Universität Karlsruhe, D-76128 Karlsruhe.

^{||} Present address: Physikalisches-Chemisches Institut, Winterthurerstr. 190, Universität Zürich, CH-8057 Zürich.

(1) Gordalla, B. C.; Zeidler, M. D. *Mol. Phys.* **1986**, *59*, 817–828.

(2) Dixit, S.; Crain, J.; Poon, W. C. K.; Finney, J. L.; Soper, A. K. *Nature* **2002**, *416*, 829–832.

(3) Kirchner, B.; Searles, D. J.; Dyson, A. J.; Vogt, P. S.; Huber, H. *J. Am. Chem. Soc.* **2000**, *122*, 5379–5383.

(4) Huber, H.; Kirchner, B.; Searles, D. J. *J. Mol. Liquids* **2002**, *98–99*, 71–77.

(5) Martin, D.; Hauthal, H. G. *Dimethylsulfoxide*; Akademie Verlag: Berlin, 1971.

0.2 in contrast to the above experiment by GZ. Various experiments, calculations and computer simulations have been carried out on water/DMSO mixtures in recent years,^{6–24} but the results obtained have not yet led to definitive conclusions regarding the composition dependence of its structure.

The main part of this work (see results in section 3.1) is devoted to calculation of relaxation times and $DQCC$ s using an approach where a precalculated efg surface is used in the simulations. As well as allowing the relaxation times to be calculated, this approach allows the $DQCC$ to be obtained with much higher statistical accuracy than has been previously obtained.³ However, the $DQCC$ will still depend on the potential chosen for the simulation.^{3,4} In a second approach (section 3.2), two recent findings of other authors^{25,26} will be combined to obtain completely independent results for the composition dependence of the $DQCC$. In Section 3.3, alternative experimental data are combined with the experimental deuteron relaxation times of GZ to get again partially independent, new results. Finally, the uncertainties of the presented results and the experimental results by GZ are analyzed and discussed (section 3.4).

2. Methods and Calculations

2.1. NMR Background. A typical experimental approach for obtaining $DQCC$ s in liquids is the measurement of NMR relaxation times, which are related to the rotational correlation time via the $DQCC$. The basic equation under the extreme narrowing regime is

$$\frac{1}{T_1} = \frac{3}{2}\pi^2 \cdot DQCC^2 \tau_2 \quad (1)$$

where the asymmetry is assumed to be small and τ_2 is a rotational correlation time of the molecule under investigation. Equation 1 is obtained from the fundamental relationship for the relaxation time under extreme narrowing conditions

$$\frac{1}{T_1} = \pi^2 \left(\frac{eQ}{h} \right)^2 \langle \mathbf{V}(0) : \mathbf{V}(0) \rangle \tau_{\text{efg}} \quad (2)$$

where eQ is the electric quadrupole moment of the deuteron, $\mathbf{V}(t)$ is the electric field gradient tensor at time t , $\langle \dots \rangle$ denotes an ensemble

- (6) Vaisman, I. I.; Berkowitz, M. L. *J. Am. Chem. Soc.* **1992**, *114*, 7889–7896.
 (7) Soper, A. K.; Luzar, A. *J. Chem. Phys.* **1992**, *97*, 1320–1331.
 (8) Luzar, A.; Chandler, D. *J. Chem. Phys.* **1993**, *98*, 8160–8173.
 (9) Ludwieg, R.; Farrar, T. C.; Zeidler, M. D. *J. Phys. Chem.* **1994**, *98*, 6684–6687.
 (10) Soper, A. K.; Luzar, A. *J. Phys. Chem.* **1996**, *100*, 1357–1367.
 (11) Hawlicka, E. *Polish J. Chem.* **1996**, *70*, 821–827.
 (12) Borin, I. A.; Skaf, M. S. *J. Chem. Phys.* **1999**, *110*, 6412–6420.
 (13) Skaf, M. S. *J. Phys. Chem. A* **1999**, *103*, 10719–10729.
 (14) Vishnyakov, A.; Lyubartsev, A. P.; Laaksonen, A. *J. Phys. Chem. A* **2001**, *105*, 1702–1710.
 (15) Cabral, J. T.; Luzar, A.; Teixeira, J.; Bellissent-Funel, M. C. *J. Chem. Phys.* **2000**, *113*, 8736–8745.
 (16) Cabral, J. T.; Luzar, A.; Teixeira, J.; Bellissent-Funel, M. C. *Physica B* **2000**, *276–278*, 508–509.
 (17) Wiewior, P. P.; Shirota, H.; Castner, E. W., Jr. *J. Chem. Phys.* **2002**, *116*, 4643–4654.
 (18) Kirchner, B.; Reiher, M. *J. Am. Chem. Soc.* **2002**, *124*, 6206–6215.
 (19) Kirchner, B.; Hutter, J. *Chem. Phys. Letts* **2002**, *364*, 497–502.
 (20) Chalaris, M.; Samios, J. *J. Mol. Liquids* **2002**, *98–99*, 399–409.
 (21) Chang, H.-C.; Jiang, J.-C.; Feng, C.-M.; Yang, Y.-C.; Su, C.-C.; Chang, P.-J.; Lin, S.-H. *J. Chem. Phys.* **2003**, *118*, 1802–1807.
 (22) Skaf, M. S.; Vecchi, S. M. *J. Chem. Phys.* **2003**, *119*, 2181–2187.
 (23) Nieto-Draghi, C.; Avalos, J. B.; Rousseau, B. *J. Chem. Phys.* **2003**, *119*, 4782–4789.
 (24) Lei, Y.; Li, H.; Han, S. *Chem. Phys. Letts* **2003**, *380*, 542–548.
 (25) Mizuno, K.; Imafuji, S.; Ochi, T.; Ohta, T.; Maeda, S. *J. Phys. Chem. B* **2000**, *104*, 11 001–11 005.
 (26) Ropp, J.; Lawrence, C.; Farrar, T. C.; Skinner, J. L. *J. Am. Chem. Soc.* **2001**, *123*, 8047–8052.

average, the colon indicates the internal tensor product and τ_{efg} is

$$\tau_{\text{efg}} = \int_0^\infty \frac{\langle \mathbf{V}(0) : \mathbf{V}(t) \rangle}{\langle \mathbf{V}(0) : \mathbf{V}(0) \rangle} dt \quad (3)$$

Equation 1 is derived from eq 2 under the assumptions that the efg correlation time τ_{efg} equals the second-order Legendre polynomial rotational correlation time τ_2 of the OD-bond vector. This is the case if intermolecular contributions and molecular flexibility do not influence τ_{efg} and if the asymmetry parameter η of the efg is zero (or if the rotation is isotropic). None of the assumptions is accurately fulfilled in the present case.²⁷

Defining the $DQCC_{\text{efg}}$ as $DQCC_{\text{efg}}^2 = (2/3)(eQ/h)^2 \langle \mathbf{V}(0) : \mathbf{V}(0) \rangle$, eq 2 becomes

$$\frac{1}{T_1} = \frac{3}{2}\pi^2 \cdot DQCC_{\text{efg}}^2 \tau_{\text{efg}} \quad (4)$$

In this definition, the effect of the asymmetry η (which is small for the efg of the deuteron of liquid water) is fully incorporated in $DQCC_{\text{efg}}$ (for a discussion see ref 27).

2.2. Fit of an Analytical Surface to the Quantum Chemically Calculated efg. In the following, D_i is used for the deuterium atom of molecule i , at which the efg is calculated. The other deuterium atom on the same molecule is denoted D'_i and O_i is the oxygen of that molecule. A second index, j indicates additional water molecules which influence the efg at D_i . In ref 28 it has been shown that the ab initio calculation of the efg tensor \mathbf{V}_i for a deuteron centered in a cluster of heavy water and DMSO molecules may be simplified using a pair approximation:

$$\mathbf{V}_i = \mathbf{V}_i^{\text{mono}} + \sum_{j \neq i} \mathbf{V}_{ij}^{\text{dim}} \quad (5)$$

$\mathbf{V}_i^{\text{mono}}$ is the efg tensor calculated for the deuterium atom in the isolated central monomer i . If \mathbf{V}_{ij} is the efg at D_j in the dimer with molecule j , the dimer contribution is defined as $\mathbf{V}_{ij}^{\text{dim}} = \mathbf{V}_{ij} - \mathbf{V}_i^{\text{mono}}$. The error made by the pair approximation is small compared to the sum of other errors in the ab initio calculation. Analytical functions that describe the monomer efg tensor as a function of the monomer configuration have been published in our paper on water.²⁷ In addition, the water–water dimer contribution was described there. It was found that with a site–site concept, simple and accurate fits to the functions are obtained rapidly. Each atom of molecule j was considered as a site A_j contributing independently to the efg tensor at D_i

$$\mathbf{V}_{ij}^{\text{dim}} = \mathbf{V}^O(O_j) + \mathbf{V}^D(D_j) + \mathbf{V}^D(D'_j) \quad (6)$$

For the two deuterium atoms D_j and D'_j , the same functions \mathbf{V}^D were used. Although the tensor is traceless, the three diagonal components were treated separately, paralleling our monomer treatment. Each of the twelve functions, that is the three diagonal elements $V_{\alpha\alpha}$ and the three off-diagonal elements $V_{\alpha\beta}$ for both \mathbf{V}^O and \mathbf{V}^D , was split into the product of a function describing the distance dependence (p^A) and a function describing the angular dependence $f_{\alpha\beta}^A(\theta_A, \Phi_A)$

$$V_{\alpha\beta}^A = p^A(r_A^{-1}) f_{\alpha\beta}^A(\theta_A, \Phi_A) \quad (7)$$

where A can be O or D . The $p^A(r_A^{-1})$ are polynomials in the inverse of the $r_A = D_i A_j$ distances. This makes sure that the dimer contributions decay to zero for large distances. For details of this function, see our previous paper.²⁷

The same procedure was applied here for the water/DMSO dimer. The O , S , and C nuclei of the DMSO molecule were used as sites A . Again for the two different carbon nuclei C and C' the same function

(27) Hardy, E. H.; Müller, M. G.; Vogt, P. S.; Bratschi, C.; Kirchner, B.; Huber, H.; Searles, D. *J. Chem. Phys.* **2003**, *119*, 6184–6193.

Table 1. Simulated NMR Data, Diffusion Coefficients and OD-Bond Lengths for Different Mole Fractions of a Water/DMSO Mixture^a

x_{water}	τ_2 /ps	τ_{efg} /ps	$DQCC_{\text{qexp}}$ kHz	$DQCC_{\text{efg}}$ kHz	R_1 /s ⁻¹	$D \cdot 10^9$ (m ² s ⁻¹)	OD-bond length/pm
1.00	0.66 (1)	0.59 (1)	252 (1)	267.3 (1)	0.62 (1)	5.45 (8)	97.32 (1)
0.95	0.82 (3)	0.73 (1)	253 (2)	267.9 (2)	0.78 (1)	4.42 (1)	97.32 (1)
0.80	1.12 (2)	1.02 (4)	257 (5)	268.8 (2)	1.09 (4)	3.27 (9)	97.27 (1)
0.65	1.40 (7)	1.23 (3)	255 (6)	270.8 (4)	1.34 (3)	2.68 (8)	97.23 (1)
0.50	1.56 (5)	1.44 (6)	261 (3)	271.8 (2)	1.58 (10)	2.38 (9)	97.18 (1)
0.30	1.64 (4)	1.46 (4)	261 (6)	276.4 (1)	1.65 (5)	2.34 (2)	97.06 (1)

^a Numbers in parenthesis are standard deviations of the mean values obtained by averaging three batches.

was applied. The fits obtained for the different tensor-components are given in the Supporting Information. They have an accuracy of better than 1 kHz.

2.3. Simulations. Molecular dynamics simulations (NVE ensemble) with a flexible water model (TIP3P²⁹/Dang-Pettitt³⁰) and a rigid DMSO model by Rao and Singh⁶ were performed for 500 molecules using the Verlet algorithm. Standard combination rules were used for the water/DMSO interactions. The simulation parameters were the same as given in ref 3, if not otherwise stated below. All densities correspond to the experimental density at ambient conditions as given in Table 1 of ref 3. Cutoff radii were given in the same table and long-range forces were treated by the Ewald summation. The reparametrization of the TIP3P potential for use with the Ewald sum suggested by Feller et al.³¹ has no consequences of importance for the present work, as our goal is not primarily to gain good absolute agreement with experiment, but rather to use a consistent model.

Special care was taken to ensure the equilibration of all degrees of freedom to the specified temperature. The motion of the water molecules was initialized by inducing normal mode vibrations in each of the monomers. The molecules were randomly orientated in space. Independent rescaling of translational, vibrational, and rotational temperature during the equilibration steps brought the system into equilibrium after several hundred thousand steps of length 0.25 fs. The three temperatures were tested independently when checking for equilibration.

Simulations were performed for water mole fractions of $x_{\text{water}} = 1.0, 0.95, 0.8, 0.65, 0.5,$ and 0.3 . For each mole fraction, 3 simulations (8 for pure D₂O) of 288 000 steps (300 000 for $x_{\text{water}} = 0.8$ and 360 000 for $x_{\text{water}} < 0.8$) were carried out to yield an average and standard deviation of this mean for all calculated values. In the results below, the standard deviations of the means for each set of simulations are given in parentheses and represent the magnitude of the error in the last digit of the value. Long simulations were needed to obtain accurate results for the slowly decaying time correlation functions. Correlation-window lengths were adjusted to be optimal for every mole fraction. The average temperature in the simulations was 301 ± 2.5 K. The simulations were performed with the SHAKE algorithm to constrain the rigid DMSO molecules.

3. Results and Discussion

As we will mostly discuss the results for $DQCC$ s, it is useful to rearrange eq 1 as follows

$$DQCC = \sqrt{\frac{2}{3\pi^2}} \frac{1}{\sqrt{\tau_2 T_1}} = \sqrt{\frac{2}{3\pi^2}} \sqrt{\frac{R_1}{\tau_2}} \quad (8)$$

where R_1 is the relaxation rate. The way in which $DQCC$ changes with mole fraction evidently depends sensitively on

(28) Müller, M. G.; Kirchner, B.; Vogt, P. S.; Huber, H.; Searles, D. J. *Chem. Phys. Letts* **2001**, *346*, 160–162.

(29) Jorgensen, W. L.; Chandrasekhar, J.; Madura, J. D. *J. Chem. Phys.* **1983**, *79*, 926–935.

(30) Dang, L. X.; Pettitt, B. M. *J. Phys. Chem.* **1987**, *91*, 3349–3354.

(31) Feller, S. E.; Pastor, R. W.; Rojnuckarin, A.; Bogusz, S.; Brooks, B. R. *J. Phys. Chem.* **1996**, *100*, 17 011–17 020.

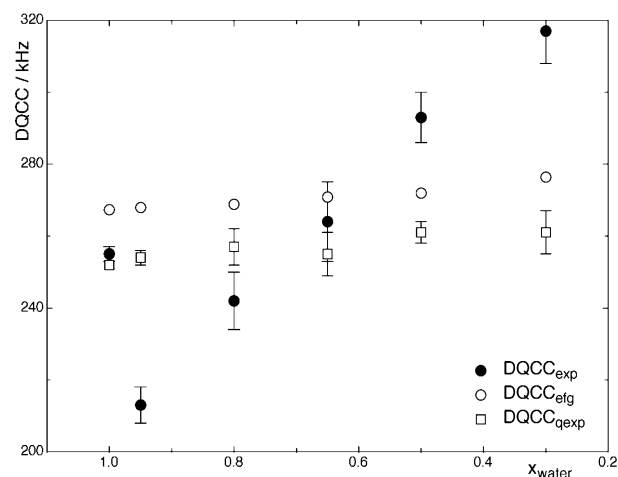


Figure 1. Deuteron quadrupole coupling constants vs the mole fraction of water in the water/DMSO mixture from GZ (black circles), from the present simulations (open circles) and including approximations used by the experimentalists (open squares). The error bars show the standard errors and are too small to be visible for the open circles.

the change of the relaxation rate relative to the change of the correlation time. Neither the relaxation rate or the correlation time change linearly with the mole fraction because the mixture is highly nonideal, and as we will show, both experimental curves pass through a maximum roughly at $x_{\text{water}} = 0.6$, as does the viscosity. A dip in the $DQCC$ as the composition changes can be realized if, for example, the correlation time function has its maximum at smaller concentrations of DMSO than the relaxation rate curve. The correlation time then increases faster at low DMSO concentrations than the relaxation rate, which leads to an initial decrease of the $DQCC$. Later, the correlation time will level off to reach its maximum, while the relaxation rate curve still increases, leading to an increase of the $DQCC$ as seen for the experimental values at higher DMSO concentrations. If the mixture is ideal, or if the two curves are proportional, the $DQCC$ will stay constant.

3.1. Simulations with a Precalculated efg Surface. The simulation approach used here not only allows calculation of dynamic properties that can directly be compared to experiment, but it enables model calculations to be carried out. These allow us to examine the errors experimentalists introduce to their results by invoking the assumptions discussed in section 2.1, which permit use of eq 1 instead of eq 2. In the simulations we obtain τ_{efg} and $\langle \mathbf{V}(0) : \mathbf{V}(0) \rangle$, and therefore using eq 2, $1/T_1$ is determined. However, we also obtain τ_2 from the same model simulation, and therefore we can use eq 1 to calculate $DQCC$ in the same way it is obtained by the experimentalists. We call $DQCC$ obtained in this way “quasi-experimental” and use the abbreviation $DQCC_{\text{qexp}}$. From eqs 1 and 2 we find the following relation

$$DQCC_{\text{qexp}} = DQCC_{\text{efg}} \cdot \sqrt{\frac{\tau_{\text{efg}}}{\tau_2}} \quad (9)$$

In Table 1 the NMR related properties, the diffusion coefficients and the average OD-bond lengths are listed to show how they depend on the composition of the mixture. The numbers given in parentheses are standard errors determined from averaging the corresponding properties of the 3 batches.

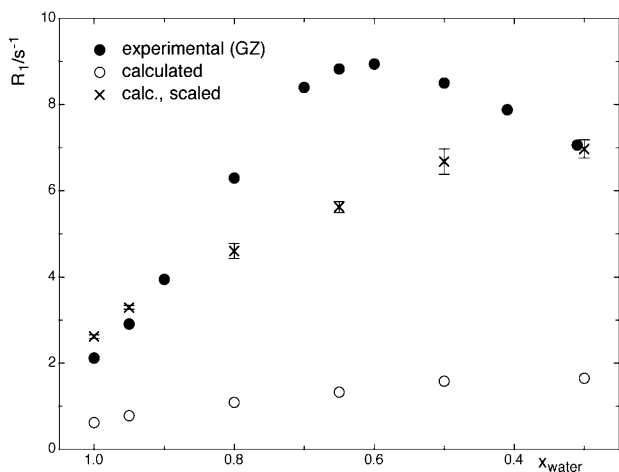


Figure 2. Deuteron relaxation rates at 298 K vs the mole fraction of water in the water/DMSO mixture. Calculated results (this work) are compared with the experimental (GZ) data. The scaled values were determined by scaling the calculated values to match the experimental (GZ) value at $x_{\text{water}} = 0.3$. The error bars show the standard errors and are too small to be visible for the open circles.

Figure 1 compares the experimental $DQCC_{\text{exp}}$ from GZ (black circles) with the $DQCC_{\text{efg}}$ from simulations (open circles), and the quasi-experimental results from eq 9 (open squares). The results from GZ are the averaged values for $T = 278, 288,$ and 298 K with the corresponding standard error. This should not introduce significant errors as the $DQCC$ shows only a very small temperature dependence. The large standard errors observed for $DQCC_{\text{qexp}}$ are due to the relatively large errors of the correlation times in eq 9.

The values for the $DQCC$ obtained from simulations show that using τ_2 instead of τ_{efg} (as is done in the experiment) produces results that are about 15 kHz or 6% too low. However, although $DQCC_{\text{qexp}}$ is lower than $DQCC_{\text{efg}}$, the $DQCC$ values obtained by using the two different calculation strategies show a remarkably parallel trend with increasing DMSO content. So, at least for our potential, accounting for the approximations used in the experiment does not help to reconcile the experimental and the simulated $DQCC$.

As shown in Figure 2, the quadrupolar relaxation rates determined from the potential used in the simulations are much too small (for a discussion of results for pure water, see ref 27). The approximate agreement in magnitude of the experimental $DQCC$ s and calculated $DQCC$ s (see Figure 1) is not observed for relaxation rates, which in accord with our previous work indicates that the structural properties are better represented by this potential than are dynamic properties.²⁷ To make a comparison easier, we have scaled the simulated relaxation rates by a factor of 4.2 to reproduce the interpolated experimental value at $x_{\text{water}} = 0.3$. The scaled values (crosses) in Figure 2 show that the simulated mixture is nonideal, but to a lower extent than is indicated by experiment. A maximum in the relaxation rates, also observed experimentally for the viscosity,³² is not obtained in the simulated results, at least not up to $x_{\text{water}} = 0.3$. It is interesting, however, that the scaled relaxation rates at small concentrations of DMSO ($x_{\text{water}} = 1.0$ and $x_{\text{water}} = 0.95$) are well reproduced and that the change from neat water to $x_{\text{water}} = 0.95$ shows about the same increase in the simulated and

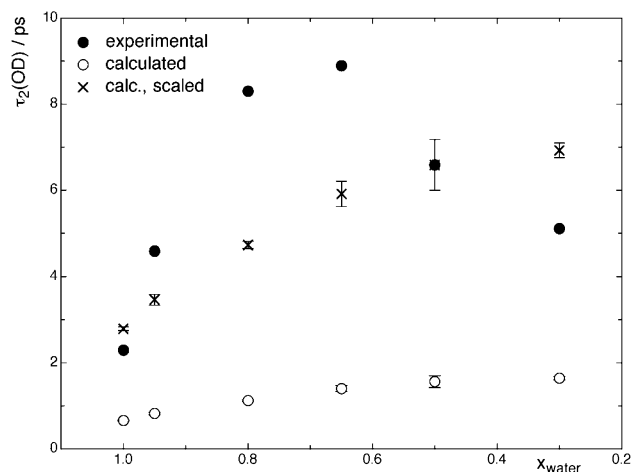


Figure 3. Rotational correlation times for D_2O at 298 K vs the mole fraction of water in the water/DMSO mixture. The scaled values are multiplied with the factor obtained in the scaling of the relaxation rates (see caption of Figure 2). The error bars show the standard errors.

experimental results. From this, we might conclude that the main difference at $x_{\text{water}} = 0.95$, i.e., where the experimental results for the $DQCC$ shows a dip, is not due to the relaxation rate, but to the correlation time (see eq 8).

Figure 3 compares simulated (open circles) and experimental (black circles) rotational correlation times. The latter were obtained from Table 5 of GZ by division with the correction factor in Table 4.¹ There is a similar absolute error in this dynamic property as found for the relaxation rate. We used the same scaling factor as for the relaxation times in Figure 2 to get the scaled values (crosses) for comparison. Again we find a nonideal behavior and again the simulated mixture is much closer to ideality than the experimental values indicate. However, the maximum in the experimental curve for the rotational correlation time occurs at higher mole fractions than the experimental maximum in the relaxation time. Furthermore, the experimental curve for the rotational correlation time shows a much steeper increase from $x_{\text{water}} = 1.0$ to $x_{\text{water}} = 0.95$ than the scaled simulated curve, although the absolute values are in fair agreement. It is evidently this discrepancy in the rotational correlation times which leads to the discrepancy in $DQCC$ at $x_{\text{water}} = 0.95$ between simulated (no dip) and experimental curves (dip).

According to the Stokes–Einstein and Stokes–Einstein–Debye relations, the rotational correlation times should be proportional to the inverse of the translational self-diffusion coefficients (D) at various water/DMSO compositions. In Figure 4 this is shown to be the case for our system.

The water/DMSO mixtures with high DMSO content ($x_{\text{water}} = 0.3, x_{\text{water}} = 0.5$) give high values of $1/D$ and long correlation times, while the lowest $1/D$ value and shortest correlation time is obtained for pure water. We will discuss this behavior in more detail in section 3.3.

Table 1 also shows the OD-bond length as a function of composition. As this bond length changes very little and smoothly, it is not surprising that the simulations yield no dip for the $DQCC_{\text{efg}}$ at $x_{\text{water}} = 0.95$. It is well-known that the $DQCC$ depends strongly on this bond length, which is in turn dependent on the strength of the hydrogen bond. The hydrogen bond between water and the O of DMSO has been found to be strong^{15,18} which might be expected to reduce the OD-bond

(32) Aminabhavi, T. J.; Gopalakrishna, B. *J. Chem. Eng. Data* **1995**, *40*, 856–861.

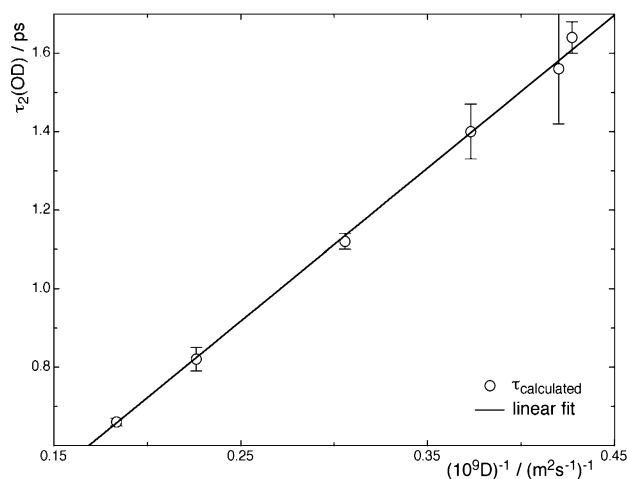


Figure 4. Calculated rotational correlation times at 298 K vs calculated inverse diffusion coefficients of water in the water/DMSO mixture. The line is a linear regression that passes through zero within two standard deviations. The error bars show the standard errors of the corresponding values. If the calculated values are replaced by the experimental values, large deviations from proportionality occur.

length in the water molecule involved in the bond. However, the trend observed in the change in the average bond length is not unexpected since fewer hydrogen bonds are formed when the concentration of DMSO increases (see, for example ref 8) due to the large volume occupied by the methyl groups.

3.2. Independent Results from a Combination of Work Published by Other Groups. Mizuno et al.²⁵ have measured proton chemical shifts for water/DMSO mixtures. These can be used in a recent relation by Ropp et al.,²⁶ developed at a molecular level from quantum chemical calculations, which correlates proton chemical shifts with deuteron quadrupole coupling constants. Here, we use eq 2 from the work of Ropp et al.²⁶

$$DQCC/\text{kHz} = -15.97 \Delta/\text{ppm} + 309.88 \quad (10)$$

where Δ is the proton chemical shift in ppm, relative to a water monomer, i.e.

$$\Delta = \sigma(\text{H}_2\text{O}) - \sigma(\text{H}_2\text{O}; \text{monomer}) \quad (11)$$

and σ is the chemical shielding. Mizuno et al.²⁵ measured their proton chemical shifts δ relative to TMS, i.e.

$$\delta = \sigma(\text{H}_2\text{O}) - \sigma(\text{TMS}) \quad (12)$$

Substituting $\sigma(\text{H}_2\text{O})$ from eq 12 into eq 11 yields

$$\Delta = \delta + \sigma(\text{TMS}) - \sigma(\text{H}_2\text{O}; \text{monomer}) \quad (13)$$

Substituting this into eq 10 we obtain

$$DQCC/\text{kHz} = -15.97 (\delta + \sigma(\text{TMS}) - \sigma(\text{H}_2\text{O}; \text{monomer}))/\text{ppm} + 309.88 = -15.97 \delta/\text{ppm} + c \quad (14)$$

where c is a constant. As we are mainly interested in relative values in the $DQCC$, we calibrate this constant by setting $DQCC = 267.3$ kHz for pure water (our value obtained from simulations) and using $\delta = 4.87$ ppm (the experimental value obtained by Mizuno et al.²⁵), which yields $c = 345.1$. Thus, we get a

Table 2. Comparison of the $DQCC$ s Obtained from Eq 15 Using Chemical Shifts δ By Mizuno et al.,²⁵ with the $DQCC$ s Obtained in the Present Simulations^a

x_{water}	δ /ppm	$DQCC/\text{kHz}$ from eq 15	$DQCC/\text{kHz}$ from simulations	$\tau_2(\text{D}_2\text{O})$ /ps ^b
1.00	4.87	267.3	267.3	2.20
0.95	4.92	266.5	267.9	3.04
0.80	4.84	267.8	268.8	6.51
0.65	4.63	271.2	270.8	8.91
0.50	4.37	275.3	271.8	8.32
0.30	4.02	280.9	276.4	6.55

^a Scaled $DQCC$ s obtained from eq 15 were combined with the experimental relaxation rates to yield the probably best values for $\tau_2(\text{D}_2\text{O})$ for this mixture (see text). ^b Calculated from T_1 by GZ and the $DQCC$ from eq 15, calibrated on neat water to 255 kHz.

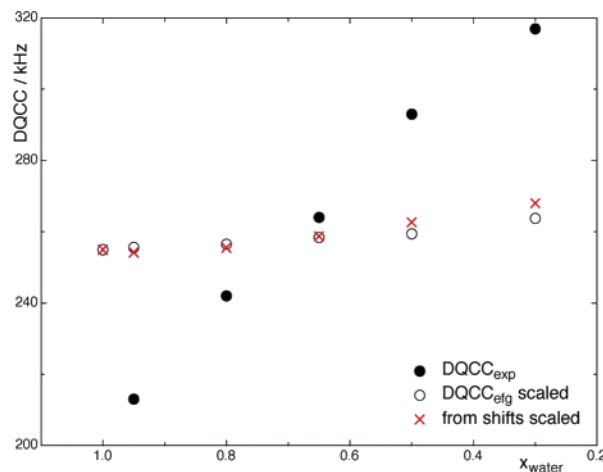


Figure 5. Deuteron quadrupole coupling constants vs the mole fraction of water in the water/DMSO mixture from GZ (black circles), from the present simulations (open circles) and from eq 15, i.e., based on the work of Mizuno et al.²⁵ and Ropp et al.²⁶ (red crosses). All values are scaled to fit the experimental (GZ) value at $x_{\text{water}} = 1$.

relation that permits calculation of quadrupole couplings from the shift measurements of Mizuno et al. to be compared with our values

$$DQCC/\text{kHz} = -15.97 \delta/\text{ppm} + 345.1 \quad (15)$$

The results are given in Table 2. The shift values were obtained from Figures 3 and 5 of Mizuno et al.²⁵ We estimate the error to be 0.02 ppm, resulting in an error of 0.3 kHz for the couplings obtained from eq 15. The error from eq 10 is not included in this estimate, as it is not given by Ropp et al.,²⁶ but the range of the chemical shifts δ is quite small (see Table 2); hence this contribution would be nearly constant for the systems considered here and is therefore not important for this analysis. Another error source could be the fact that eq 10 was found from pure water clusters, while the present investigation concerns a mixture. However, Farrar and co-workers have shown in additional publications that linear regressions with very similar slope are valid for methanol/ CCl_4 mixtures³³ and ethanol mixed with several solvents, e.g., DMSO.³⁴ Hence, at least for the low concentrations of DMSO, i.e., at the position of the experimental dip in the $DQCC$ that we are examining, the relation should be accurate, whereas at higher concentrations of DMSO a slight deviation could be the reason for the small

(33) Wendt, M. A.; Farrar, T. C. *Mol. Phys.* **1998**, *95*, 1077–1081.

(34) Ferris, T. D.; Zeidler, M. D.; Farrar, T. C. *Mol. Phys.* **2000**, *98*, 737–744.

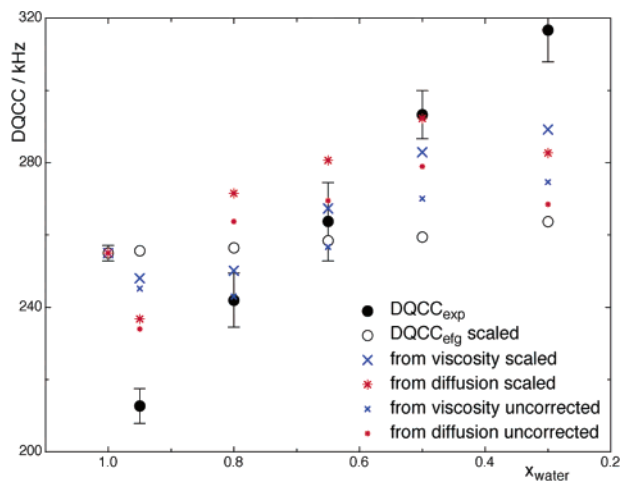


Figure 6. Deuteron quadrupole coupling constants vs the mole fraction of water in the water/DMSO mixture from GZ (black circles), from the present simulations (open circles), from experimental viscosities (see text, blue crosses), and from experimental diffusion coefficients (see text, red stars). All values are scaled to fit the experimental (GZ) value at $x_{\text{water}} = 1$.

disagreement between the results obtained from the measurement of Mizuno et al.²⁵ and our simulated values. Figure 5 shows all results scaled to the GZ value for neat water.

The results determined using eq 15 show a small dip at $x_{\text{water}} = 0.95$ of -0.8 kHz. However this is negligible compared to the value by GZ of -42 kHz. Overall there is an excellent agreement with our data, which are thus confirmed by this completely independent work where no empirical potential was used.

In the last column of Table 2 rotational correlation times for D_2O are listed, which were obtained from the quadrupole relaxation rates by GZ and the $DQCC$ s from eq 15, scaled to the experimental value of 255 kHz for neat water (which is in good agreement with our result of 252 kHz for $DQCC_{\text{qexp}}$). Considering that the relaxation rates and chemical shifts can be accurately measured, and that the quantum chemical calculations were performed on a high level, they are probably the best available values for τ_2 of D_2O in this mixture (still assuming a concentration independence of τ_2/τ_{efg}).

3.3. Combination of Other Experiments from the Literature with the Deuteron Relaxation Rates of Gordalla and Zeidler. Assuming the proportionality of τ_2 to the viscosity or inverse translational self-diffusion coefficient mentioned in 3.1, we can make further determinations of the change in the $DQCC$ with composition using experimental results. Although the Stokes–Einstein and Debye relations have been developed for macroscopic objects it has been found that they can also be applied to molecular systems. We confirmed this in the present case in Figure 4, where the proportionality between τ_2 and the inverse translational self-diffusion coefficient holds for the model used in our simulations. In addition, Cabral et al.¹⁵ showed that an eutectic mixture of 2 water/1 DMSO follows the Stokes–Einstein relation between shear viscosity and diffusion coefficient for different temperatures.

Using the proportionality of the inverse translational diffusion coefficient or the shear viscosity to τ_2 , we can determine the trends in the $DQCC$ by introducing experimental results for the viscosity or the inverse diffusion coefficient in eq 8. For a comparison we scaled these values to the experimental GZ value for neat water. The results shown in Figure 6 were obtained

from viscosities by Aminabhavi et al.³² (the results are nearly the same as the older values by Cowie and Toporowski³⁵) and diffusion coefficients by Packer and Tomlinson.³⁶

As the values in the literature were obtained for $\text{H}_2\text{O}/\text{DMSO}$, they have to be corrected for the higher viscosity and lower translational self-diffusion coefficients in $\text{D}_2\text{O}/\text{DMSO}$, corrections that become less important with decreasing water content. We use the correction factors derived by GZ from relaxation measurements in $\text{H}_2\text{O}/\text{D}_2\text{O}/\text{DMSO}$ mixtures (Table 4 in ref 1). In Figure 6 the uncorrected values (for H_2O) are also shown. At $x_{\text{water}} = 0.95$ we can see a dip in both curves, however its size is reduced by a factor two (diffusion) to four (viscosity) compared to the experimental results of GZ. The curves obtained from diffusion (red stars) then rise steeply above our simulated values at $x_{\text{water}} = 0.8$ and stay always slightly above. At $x_{\text{water}} = 0.3$ they clearly differ from the GZ values, and are significantly higher than our values. The error given by Packer and Tomlinson in that region is about 10%, which yields about 5% or 14 kHz for the $DQCC$. The curves obtained from viscosity (blue crosses) also show dips, but they follow our simulated values more closely. The experimental error given by Aminabhavi and Gopalakrishna for the viscosities is negligible for the present discussion. The uncorrected curves deviate from the corrected curves as the dynamic isotope effect is evidently concentration dependent. Interestingly, the uncorrected values show a much better agreement with our values for the smaller mole fractions. One should note that the relaxation rate used for calculation of the $DQCC$ s shown in Figure 6 (via eq 8) are those from the GZ work, so these data are not fully independent in contrast to those in Figure 5.

3.4. Discussion of Possible Error Sources. From the discussion at the beginning of this paper it is clear that an evaluation of the $DQCC$ by eq 8 is sensitive to the functional form of the relaxation rate and the correlation time. We do not expect the simulated curves to be quantitatively correct since the potential is imperfect, and indeed the relaxation rates and correlation times are by more than a factor four out. However, the $DQCC$ is a structural property and we would assume that the simulations in section 3.1 should produce results for structural properties with reasonable accuracy (in accord with e.g., Lei et al.²⁴ and Luzar et al.,⁸ who conclude that for these systems the structure is “seemingly invariant to reasonable changes to the intermolecular potential” and further state that “in the mixing process, hydrogen bonding is simply transferred from water–water interactions to water/DMSO interactions”). Our previous work has also shown that the $DQCC$ in bulk water is insensitive to the potential energy surface and the choice of parameters used in the calculations in this work are sufficient to produce accurate results.^{3,37} As the $DQCC$ is a structural property, eq 8 shows how the relaxation and the correlation times are coupled. Only if $DQCC$ is evaluated through these times, which is not the case in the simulations, should it be sensitive to these properties. Therefore, we would expect that the simulations should give the qualitatively correct result, but might deviate slightly quantitatively. That is, we would expect the large dip in $x_{\text{water}} = 0.95$ observed by GZ to be observed in the simulated results, if it is a real effect. The discussion in

(35) Cowie, M. G.; Toporowski, P. M. *Can. J. Chem.* **1964**, *39*, 224.

(36) Packer, K. J.; Tomlinson, D. J. *Trans. Faraday Soc.* **1971**, *67*, 1302–1314.

(37) Eggenberger, R.; Gerber, S.; Huber, H.; Searles, D. J.; Welker, M. J. *Comput. Chem.* **1993**, *14*, 1553.

section 3.1 would then suggest that we have to look for an error in the experimental evaluation of the rotational correlation time.

Similarly, the evaluation from the chemical shifts in section 3.2 should not be sensitive to any dynamic properties. As the results were obtained completely independently of the earlier experimental work and our simulations, they are a strong confirmation of our simulation results. Of course the small dip seen in the trend determined from chemical shift measurements shown in Figure 5 could be an underestimation, but even if it were slightly larger, it is far from reproducing the GZ results. Similarly, the deviations of the results in 3.2 from the simulated results at smaller mole fractions are small and deviate in a qualitative manner from the GZ values.

The results in section 3.3 were obtained from dynamic properties. They are not independent of the GZ values as the GZ relaxation rates and also their correction factors for the corrected values were used. This shows again how sensitive the $DQCC$ s are to the correlation times. Of course one has to keep in mind that several assumptions were made in obtaining these correlation times and they are not directly obtained. The correlation times τ_2 are determined by GZ indirectly using an extrapolation of relaxation rates, and viscosity corrections for isotopes (^{16}O , ^{17}O , ^{18}O , ^1H , ^2H).¹ In a different experiment³⁸ GZ deeply cooled a water/DMSO mixture with $x_{\text{water}} = 0.68$ and thus were able to proceed beyond the extreme-narrowing region. In this way, the square of the dipolar coupling constant, needed to calculate the correlation time from the dipolar relaxation rate, can be obtained from the NMR measurements, instead of calculating it from the OH-bond distance. It is known that the square of the coupling constant derived in this manner, which is adequate for relaxation measurements, is lower than the one calculated with the equilibrium distance, due to molecular flexibility. It is this deviation which is taken into account by the generalized order parameter by Lipari and Szabo.³⁹ However, GZ surprisingly only obtained half of the value calculated in ref 1, meaning that the correlation time is doubled and the $DQCC$ would be reduced by 29%. Obviously, the dipolar relaxation of water in this mixture is not fully understood, and most probably effects not considered in the evaluation of the correlation times from dipolar relaxation lead to the unexpected behavior of the $DQCC$ found in ref 1. Simulations should be useful to analyze these effects.

The starting point for this work was to study if the assumption $\tau_{\text{efg}} = \tau_2$ could explain the discrepancy between $DQCC_{\text{exp}}$ and $DQCC_{\text{efg}}$. Indeed τ_{efg} is significantly shorter than τ_2 , leading to a decrease of $DQCC_{\text{qexp}}$ compared to $DQCC_{\text{efg}}$ by a factor of $\sqrt{\tau_{\text{efg}}/\tau_2}$, but no concentration dependence of this factor was found. Since the dynamics produced by the potential model are poor (absolutely as well as relatively for different concentrations), the uncertainty of this factor has to be discussed. In previous work,²⁷ we showed that in neat water, the different effects of molecular flexibility on τ_{efg} and τ_2 were mainly responsible for the decrease of τ_{efg} compared to τ_2 (originating in the monomer–dimer cross terms when inserting eq 5 into eq 3). Adding DMSO to water with $x_{\text{water}} = 0.9$, the viscosity and probably τ_2 also double. One can speculate that in this situation the relative influence of molecular flexibility on the decrease of the efg time correlation function is larger, leading

to a dip for $DQCC_{\text{qexp}}$, and that this effect is not correctly reproduced by the simulation. Similarly, one can speculate that for high dilution the monomer–dimer cross terms become less important, raising τ_{efg} toward τ_2 and $DQCC_{\text{qexp}}$ toward $DQCC_{\text{efg}}$ and that this effect again is not well reproduced in our simulation. Better potentials and statistics are needed to check these speculations.

We note that structural properties are not as sensitive to temperature as dynamic properties such as the relaxation and correlation times. Therefore, the evaluations in section 3.1 and 3.2 should not be sensitive to errors in temperature. However the evaluations in section 3.3 and by GZ depend on the combination of different relaxation rates or relaxation rates and other dynamic properties and are subject to significant possible errors due to small errors in the temperature.

Focusing our analysis on the rotational correlation time we found one peculiarity in its evaluation by GZ. In contrast to the deuteron-relaxation time measurement they used DMSO- d_6 . However, additional simulations performed with DMSO- d_6 did not change the above results significantly and are, therefore, excluded as possible error source.

4. Conclusions

Simulations with a precalculated electronic property surface presented here for a water/DMSO mixture permit the simultaneous calculation of $DQCC$ s, relaxation rates, efg time correlation functions and rotational correlation functions. This allows the errors introduced in the experimental evaluation of the coupling constant to be checked using a consistent model. The use of the rotational rather than the electric field gradient correlation time yields $DQCC$ s for our model that are too small by about 15 kHz for the deuterons in water. However, this effect is independent of the composition and therefore a dip at $x_{\text{water}} = 0.95$ and the steep rise at smaller mole fractions observed by Gordalla and Zeidler¹ is still not reproduced.

The new simulations confirm previous results³ with better statistics, which showed a monotonic $DQCC$ curve increasing little with dilution by DMSO. This is no surprise as the same potential was used. However, since this time experimental and theoretical results have been published in the literature, the combination of which allows a completely independent determination of the $DQCC$. They confirm the simulated results. Combinations of the GZ deuteron relaxation rates with independent diffusion and viscosity measurements yield results between the GZ and the present results, assuming the proportionality of these independent measurements and the rotational correlation time. As further experiments by GZ indicate,³⁸ effects not considered in the evaluation of correlation times from proton relaxation times probably lead to the unexpected behavior evaluated by GZ.

Acknowledgment. This work is part of the project 2000-066530.01 of the Schweizerischer Nationalfonds zur Förderung der Wissenschaften. We thank the Australian Research Council for support of this work.

Supporting Information Available: Fit-functions and coefficients for the dimer contributions to the electric field gradient tensor components. This material is available free of charge via the Internet at <http://pubs.acs.org>.

(38) Gordalla, B. C.; Zeidler, M. D. *Mol. Phys.* **1991**, *74*, 975–984.

(39) Lipari, G.; Szabo, A. *J. Am. Chem. Soc.* **1982**, *104*, 4546–4559.